J. Fluid Mech. (1970), *vol.* 44, *part* 4, *pp.* 695–704
Printed in Great Britain

Thermal convection in an infinite channel with no-slip sidewalls

By ROBERT P. DAVIES-JONES

Advanced Study Program, National Center for Atmospheric Research, Boulder, Colorado 80302 U.S.A.

(Received 10 December 1969 and in revised form 20 May 1970)

We obtain exact solutions of the linearized perturbation equations for the convective motions in a Boussinesq fluid contained in an infinite rectangular channel and heated from below. The top and bottom are assumed to be perfect heat conductors. The sides can either be conducting or insulating. We assume that the sidewalls are rigid, but allow the top and bottom to be free so that we can separate variables.

We find that the preferred modes of convection closely resemble transverse 'finite rolls' [as predicted by Davis (1967) for convection in a box] for channels with height to width ratios outside the range 0·1 to 1. Inside this range they show noticeable departures from roll form. We prove, however, that, except when the sidewalls are relaxed to infinity, 'finite rolls' are never exact solutions of the linearized equations, even though in most cases they are good approximations.

We also find that bringing the sidewalls closer together inhibits convection and, generally, produces thinner cells at the onset of convection.

1. Introduction

Linear theory predicts for an infinite layer of fluid with free boundaries heated from below, the Rayleigh number (= 657·5) and the horizontal wave-number (= 2·22 in units of the inverse of the fluid depth) at the onset of convection, but it allows an infinite spectrum of cell shapes. Non-linear effects have to be included in the theory to explain the observed shapes. The presence of lateral boundaries can also lift the degeneracy of the eigenfunctions, and permit one mode to be preferred over the others. Koschmeider (1966) has shown that the influence of lateral boundaries dominates the non-linear effects in the selection of cell shape if the width of the apparatus is an order of magnitude larger than the height.

Davis (1967) investigated the linear stability of a rigid, perfectly conducting, rectangular box of fluid heated from below. He defined 'finite rolls' as cells with two non-zero velocity components dependent on all three spatial variables, and found upper bounds to the critical Rayleigh number by using Galerkin's technique with 'finite roll' trial functions. Within his approximation general three-dimensional flows can be constructed by a linear superposition of finite rolls so that he was able to predict the preferred mode at the onset of convection. He found that the presence of sidewalls can resolve the cell shape degeneracy of the

linear thermal convection problem, and that his analysis predicted finite rolls with axes parallel to the shorter sides.

In this paper we show that the linearized solutions can never be exactly finite rolls unless the sidewalls are infinitely far apart, and we present exact solutions for convection in an infinite rectangular channel with no-slip sidewalls and free top and bottom. Our results show, however, that the cells which appear at the onset of convection resemble finite rolls very closely for channel aspect ratios (height to width) outside the range 0·1 to 1. Inside this range they show noticeable departures from roll form.

The fact that the linearized equations have near-finite roll solutions is not surprising in view of Segel's (1969) results for the non-linear problem. Segel found non-linear finite-roll solutions at sufficiently small aspect ratios.

2. Formulation of the problem

We use the following notation: x and y are the horizontal co-ordinates along and across the channel and z is the vertical co-ordinate. The subscript $*$ refers to dimensional quantities. The channel is defined by the planes $z_* = 0$, d_* and $y_* = \pm b_*$. u_*, v_* and w_* are the components of velocity in the x, y and z directions, p_* is the pressure, ρ_* is the density, θ_* is the temperature measured with respect to the average temperature, g_* is the acceleration due to gravity, and α_*, ν_* and κ_* are the coefficients of volume expansion, kinematic viscosity and thermal conductivity.

We assume that in the initial steady state there is no motion. The vertical temperature gradient, β_*, is constant as it is established solely by heat conduction.

We now introduce infinitesimal perturbations, denoted by primes, into the system. If they grow with time, the initial equilibrium is unstable. We assume that the applied temperature difference between top and bottom is small enough so that we can use the Boussinesq approximation (i.e. $|\alpha_*\theta_*| \ll 1$). We define non-dimensional variables (non-subscripted) as follows

$$\begin{aligned} x, y, z &\equiv d_*^{-1}[x_*, y_*, z_*], \\ t &\equiv \kappa_* d_*^{-2} t_*, \\ u', v', w' &\equiv d_* \kappa_*^{-1}[u'_*, v'_*, w'_*], \\ \theta' &\equiv -\beta_*^{-1} d_* \theta'_*, \\ p' &\equiv \rho_{0_*}^{-1} d_*^2 \kappa_*^{-2} p'_*, \end{aligned}$$

where ρ_{0_*} is the mean density of the fluid in the channel. The linearized perturbation equations are then

$$\mathscr{L}_1 u' = -\partial p'/\partial x, \tag{1}$$

$$\mathscr{L}_1 v' = -\partial p'/\partial y, \tag{2}$$

$$\mathscr{L}_1 w' = -\partial p'/\partial z + PR\theta', \tag{3}$$

$$\partial u'/\partial x + \partial v'/\partial y + \partial w'/\partial z = 0, \tag{4}$$

$$\mathscr{L}_2 \theta' - w' = 0, \tag{5}$$

where $\mathscr{L}_1$ and $\mathscr{L}_2$ denote the differential operators $(\partial/\partial t - P\nabla^2)$ and $(\partial/\partial t - \nabla^2)$ respectively, $P = \nu_*/\kappa_*$ is the Prandtl number, and $R = -g_*\alpha_*\beta_* d_*^4/\kappa_*\nu_*$ is the Rayleigh number.

The conditions for free, perfectly conducting top and bottom boundaries are

$$\theta' = w' = \partial u'/\partial z = \partial v'/\partial z = 0 \quad \text{at} \quad z = 0, 1. \tag{6}$$

Since the sidewalls are rigid and perfect conductors (or perfect insulators), the boundary conditions in y are

$$u' = v' = w' = \theta' (\text{or } \partial\theta'/\partial y) = 0 \quad \text{at} \quad y = \pm a, \tag{7}$$

where $a \equiv b_*/d_*$. From (4) and (5) these are equivalent to

$$v' = \partial v'/\partial y = \theta' (\text{or } \partial\theta'/\partial y) = \mathscr{L}_2\theta' = 0 \quad \text{at} \quad y = \pm a. \tag{8}$$

Unfortunately, however, these boundary conditions cannot be expressed in terms of a single variable.

3. The exchange of stabilities

Sherman & Ostrach (1966) have proved that the principle of exchange of stabilities holds (i.e. all non-decaying disturbances are non-oscillatory in time) for convection in a fully enclosed geometry. Only slight modification of their proof is needed to show that it also holds for convection in a infinite (periodic) channel, so we omit discussion of it here.

4. Proof that finite rolls are not exact solutions in linear theory

To show that finite rolls are not exact solutions of the linearized equations, we first set one of the horizontal velocity components, v', identically zero in the perturbation equations (1)–(5) and define a stream function ψ by

$$u' = -\partial\psi/\partial z, \quad w' = \partial\psi/\partial x. \tag{9}$$

Since $\partial p'/\partial y \equiv 0$ from (2) [with $v' \equiv 0$], we obtain

$$\mathscr{L}_1 \partial^2\psi/\partial y\,\partial z = 0 \tag{10}$$

and

$$\mathscr{L}_1 \partial^2\psi/\partial x\,\partial y = PR\partial\theta'/\partial y, \tag{11}$$

by differentiating (1) and (3) with respect to y. Elimination of ψ from (10) and (11) yields

$$\partial^2\theta'/\partial y\,\partial z \equiv 0. \tag{12}$$

Now, if the side-boundaries at $y = \pm a$ and the top and bottom are conducting ($\theta' = 0$ there) then $\theta' \equiv 0$. Hence, $w' \equiv 0$ from (5). Thus, convective solutions with $v' \equiv 0$ are not exact solutions of (1)–(5) (except when $a = \infty$ since in this case $\partial\theta'/\partial y \equiv 0$, and $\theta' = 0$ at the sides, does not necessarily imply that $\theta' \equiv 0$).

If, on the other hand, the side-boundaries are insulating ($\partial\theta'/\partial y = 0$ at $y = \pm a$), then θ', and w' must both be independent of y from (12) and (5). However, if the boundaries are also rigid ($w' = 0$ at $y = \pm a$), then $w' \equiv 0$ and once again there is no convective solution with $v' \equiv 0$ which satisfies the boundary conditions.

Thus, finite rolls which are aligned perpendicular to conducting or insulating, rigid sidewalls do not satisfy the linearized equations exactly. Note that we have not made use of either the boundary conditions in the x direction or the kinematic conditions at the top and bottom. The proof therefore is valid for rigid, conducting boxes (as considered by Davis) as well as infinite rectangular channels.

5. The method of solution

By elimination of variables in (1)–(5) we obtain the single sixth-order differential equation in θ'

$$\nabla^2 \mathscr{L}_1 \mathscr{L}_2 \theta' - PR\nabla_H^2 \theta' = 0. \tag{13}$$

Because we cannot formulate all of the boundary conditions in terms of θ', we need the following equation which relates v' and θ'

$$\partial \mathscr{L}_1 v'/\partial z = (\mathscr{L}_1 \mathscr{L}_2 - PR)\, \partial \theta'/\partial y. \tag{14}$$

The boundary conditions (6) allow us to separate variables by assuming that

$$\left.\begin{aligned} \left.\begin{matrix} u'(x,y,z,t) \\ v'(x,y,z,t) \\ p'(x,y,z,t) \end{matrix}\right\} &= \left\{\begin{matrix} \hat{u}(y) \\ \hat{v}(y) \\ \hat{p}(y) \end{matrix}\right\} e^{\sigma t} e^{ikx} \cos mz, \\ \left.\begin{matrix} w'(x,y,z,t) \\ \theta'(x,y,z,t) \end{matrix}\right\} &= \left\{\begin{matrix} \hat{w}(y) \\ \hat{\theta}(y) \end{matrix}\right\} e^{\sigma t} e^{ikx} \sin mz, \end{aligned}\right\} \tag{15}$$

where σ is the growth rate of the normal mode disturbance with x wave-number k and vertical wave-number m ($= n\pi$; $n = 1, 2, 3, \ldots$). We assume henceforth that $n = 1$ since this gives the most unstable mode.

Substitution of (15) into (13) and (14) yields

$$P\frac{d^6\hat{\theta}}{dy^6} - \{\sigma[P+1] + 3\alpha^2 P\}\frac{d^4\hat{\theta}}{dy^4} + \{\sigma^2 + 2\sigma\alpha^2[P+1] + 3\alpha^4 P - PR\}\frac{d^2\hat{\theta}}{dy^2}$$
$$- \{\alpha^2\sigma^2 + \sigma\alpha^4[P+1] + \alpha^6 P - k^2 PR\}\hat{\theta} = 0 \tag{16}$$

and

$$m\left(P\frac{d^2}{dy^2} - P\alpha^2 - \sigma\right)\hat{v} = -\left\{P\frac{d^5}{dy^5} - [2P\alpha^2 + \sigma(1-P)]\frac{d^3}{dy^3}\right.$$
$$\left. + [(\alpha^2+\sigma^2)(P\alpha^2+\sigma^2) - PR]\frac{d}{dy}\right\}\hat{\theta}, \tag{17}$$

where $\alpha^2 = k^2 + m^2$.

Now (16) has the general solution

$$\hat{\theta}(y) = \sum_{j=1}^{6} C_j e^{r_j y}, \tag{18}$$

where the r_j are the roots of the characteristic equation of (16) and the C_j are arbitrary constants, unless two or more of the roots are equal. For the present we assume that the roots are distinct. The characteristic equation is bi-cubic with real coefficients so that the r_j can be determined using standard formulae for the roots of a cubic equation.

After substituting for $\hat{\theta}$ from (18), (17) becomes a second-order inhomogeneous differential equation in $\hat{v}$. It has a particular integral

$$\hat{v}_2(y) = \sum_{j=1}^{6} C_j \beta_j e^{r_j y}, \tag{19}$$

where the β_j are given by the formula

$$\beta_j = -\frac{1}{m} \frac{Pr_j^5 - [2P\alpha^2 + (1+P)\sigma] r_j^3 + [(\alpha^2+\sigma^2)(P\alpha^2+\sigma) - PR] r_j}{Pr_j^2 - P\alpha^2 - \sigma}, \tag{20}$$

which is obtained by the method of undetermined coefficients. The complementary function of (17) is

$$\hat{v}_1(y) = \sum_{j=7}^{8} C_j e^{r_j y}, \tag{21}$$

where

$$r_{7,8} = \pm [\alpha^2 + (\sigma/P)]^{\frac{1}{2}}. \tag{22}$$

Thus, the general solution for $\hat{v}(y)$ is

$$\hat{v}(y) = \sum_{j=1}^{6} C_j \beta_j e^{r_j y} + \sum_{j=7}^{8} C_j e^{r_j y}. \tag{23}$$

Applying the boundary conditions (8) to (18) and (23) gives us eight equations which we write in symbolic form as follows:

$$\sum_{j=1}^{8} q_{ij} C_j = 0 \quad (i = 1, 2, \ldots, 8). \tag{24}$$

where the q_{ij} are functions of r_j and β_j. For non-trivial solutions (i.e. the C_j not all zero), the determinant $|q_{ij}|$ must vanish. We find the Rayleigh number at which disturbances become marginally stable by setting $\sigma = 0$, and locating the zeros of $|q_{ij}|$ (considered as a function of R) numerically on the computer. The task is made easier by the fact that $|q_{ij}|$ is always real or purely imaginary.

Having computed the eigenvalue, R, we can find the constants $C_1, C_2, \ldots, C_7$ in terms of C_8 by means of Cramer's rule. We then have the solutions for $\hat{v}$ and $\hat{\theta}$. The solutions for the other variables may be found from the relationships

$$w' = \mathscr{L}_2 \theta', \tag{25}$$

$$u' = -(1/ik)(\partial v'/\partial y + \partial w'/\partial z), \tag{26}$$

$$p' = -(1/ik)\mathscr{L}_1 u', \tag{27}$$

which are obtained from (5), (4) and (1).

Now consider the case where the roots, r_j, of the characteristic equation are not all distinct. Since the characteristic equation is a bi-cubic, if two non-zero roots are equal, then two other roots are also equal. Suppose that

$$r_3 = r_5, \quad r_4 = r_6.$$

Then the general solution of (16) is not (18) but

$$\hat{\theta}(y) = \sum_{j=1}^{4} C_j e^{r_j y} + \sum_{j=5}^{6} C_j y e^{r_{j-2} y}. \tag{28}$$

In practice we would like to have a general solution of (16) that applies when the roots are nearly equal as well as when they are exactly equal. Ince (1956) showed that if r_i and r_j are roots of the characteristic equation, then $(e^{r_i y} - e^{r_j y})/(r_i - r_j)$ is a solution which tends to $y e^{r_i y}$ as r_i tends to r_j. That is, it has the right limiting behaviour in the limit r_i equal to r_j. Therefore, if we have two pairs of nearly equal roots, (r_3, r_5) and (r_4, r_6), we use the general solution

$$\hat{\theta}(y) = \sum_{j=1}^{4} C_j e^{r_j y} + \sum_{j=5}^{6} C_j \frac{e^{r_j y} - e^{r_{j-2} y}}{r_j - r_{j-2}}, \tag{29}$$

and proceed with the same method for finding the eigenvalues and the solutions as before.

The case of two roots being zero can be dealt with in a similar manner.

6. Finite roll calculations

We performed some calculations in which we assumed that $v' \equiv 0$ and solved the particular set of equations (1), (3), (4) and (5) (i.e. we did not take the y equation of motion into account). The differences between these results and the actual results should be a measure of the closeness of the exact solutions to finite rolls.

In this case we obtain a fourth-order differential equation in θ', namely

$$\mathscr{L}_1 \mathscr{L}_2 \nabla_1^2 \theta' - RP \partial^2 \theta' / \partial x^2 = 0, \tag{30}$$

where $\nabla_1^2 \equiv \partial^2/\partial x^2 + \partial^2/\partial z^2$. The side boundary conditions (8) reduce to

$$\left.\begin{aligned} &\theta' = \mathscr{L}_2 \theta' = 0 \quad \text{at} \quad y = \pm a \text{ for perfect conductors,} \\ &\partial\theta'/\partial y = \mathscr{L}_2 \theta' = 0 \quad \text{at} \quad y = \pm a \text{ for perfect insulators.} \end{aligned}\right\} \tag{31}$$

For insulating sides we solved this boundary-value problem by assuming the form for θ' given in (15), and using the method described in § 5. For conducting sides the solution for θ' has the simple form

$$\theta' \sim e^{\sigma t} e^{ikx} \sin mz \begin{cases} \cos(q\pi y/2a) & \text{for} \quad q = 1, 3, 5, \ldots, \\ \sin(q\pi y/2a) & \text{for} \quad q = 2, 4, 6, \ldots, \end{cases} \tag{32}$$

where $m = \pi$ for the lowest mode in the vertical. By substituting (32) into (30) and putting $\sigma = 0$ we obtain

$$R_{\sigma=0} = \frac{(k^2 + \pi^2)(k^2 + \pi^2 + (q^2\pi^2/4a^2))^2}{k^2} \tag{33}$$

at marginal stability. The critical wave-number (i.e. that value of k for which $R_{\sigma=0}$ is a minimum) is given by

$$k_c = \tfrac{1}{2}([9\pi^4 + (2\pi^4/a^2)]^{\frac{1}{2}} - \pi^2)^{\frac{1}{2}}. \tag{34}$$

7. The results

Figures 1 and 2, for conducting and insulating sidewalls respectively, show the Rayleigh numbers at which the two lowest modes become unstable as a function of k for different aspect ratios. The role of the lateral boundaries in lifting the degeneracy of the eigenfunctions is apparent from the observation that the curves for the two modes get further apart as the walls come closer together. An examination of the eigenfunctions shows that the mode which has the lower minimum is symmetric with regions of maximum updraft and downdraft in the centre of the channel. The other mode is antisymmetric. Except for $k \lesssim 1$ the symmetric mode is the more unstable of the two.

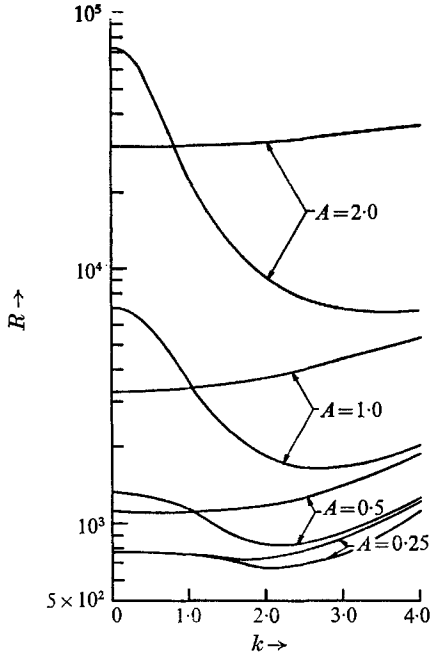

FIGURE 1

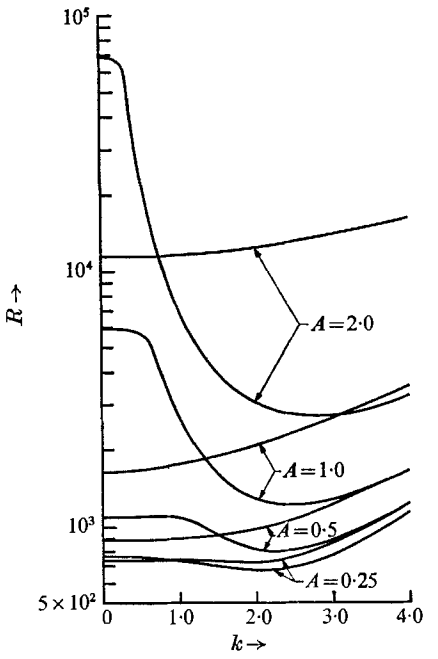

FIGURE 2

FIGURE 1. The Rayleigh numbers at which the two lowest modes are marginally stable as functions of wave-number at different aspect ratios for perfectly conducting sidewalls.

FIGURE 2. The same as figure 1 but for perfectly insulating sidewalls.

Figures 3 and 4 give the critical Rayleigh number and critical wave-number plotted against aspect ratio for conducting sides (labelled I) and for insulating sides (II). The solid lines represent exact results; the dotted ones the results of the finite roll calculations described in § 6. During our discussion of these figures we shall refer to figures 5–8 which are horizontal plan forms of the cells at the onset of convection for channels with conducting and insulating sidewalls, and aspect ratios of 0·5 and 2·0.

The higher critical Rayleigh number in the conducting case (see figure 3) is a manifestation of heat loss through the sides. The critical Rayleigh number increases with A because as the sidewalls are brought closer together the cross-

channel gradients of velocity and temperature increase, and hence the dissipation is amplified.

Notice that the finite roll calculations give values of R_c which are always too high. The errors are worst at moderately small aspect ratios ($0{\cdot}1 < A < 1{\cdot}0$). At these aspect ratios the convection departs quite markedly from roll form (see figures 5 and 7) because the establishment of a cross-channel component of

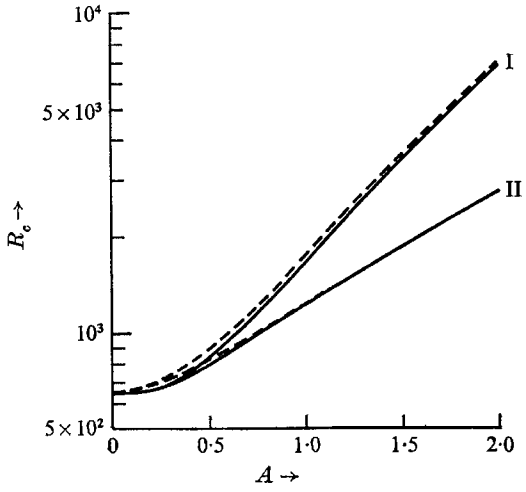

FIGURE 3

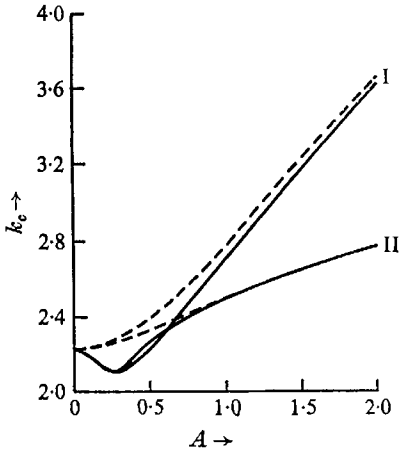

FIGURE 4

FIGURE 3. Critical Rayleigh number *versus* aspect ratio for conducting sidewalls (I) and insulating sidewalls (II). Solid lines represent the exact results; the dashed lines the results of the finite roll calculations.

FIGURE 4. Critical wave-number *versus* aspect ratio. The notation is the same as in the previous figure.

velocity enables more fluid to flow into the regions of maximum updraft and downdraft which are situated midway between the sidewalls. The cells thus become more efficient, i.e. most fluid particles have shorter cycle times, and more able to combat the increased dissipation. At large aspect ratios, the cells bear closer resemblance to finite rolls (see figures 6 and 8) because with the enhancement of the side boundary layers the fastest rising (sinking) fluid particles prefer to travel in the centre of the channel where the viscous forces are weakest when they reach the top (bottom).

Finite rolls are also better approximations to the exact solutions when the walls are insulators rather than conductors (compare figures 5 and 7 or 6 and 8). We can attribute this result to the fact that in the conducting case, where θ' has to vanish at the sides, there are stronger cross-channel temperature gradients to drive circulations in y, z planes than in the insulating case.

Figure 4 shows that as the sidewalls are moved in from infinity, the cells widen slightly at first (for $0 < A \lesssim 0{\cdot}25$) before narrowing (for $A \gtrsim 0{\cdot}25$). This widening is not a feature of the finite roll calculations so that it must be due in some way to advection across the channel. For $A \geqslant 0{\cdot}25$, k_c increases with A so that the cells can become more efficient in order to sustain themselves against rapidly increasing

dissipation. [Note that increasing k also further increases the dissipation. However, this extra dissipation is presumably outweighed here by the gain in efficiency.]

The critical wave-number is generally smaller for insulating sidewalls than for conducting ones because in the insulating case the cells do not have to increase their efficiency as much since there is no heat lost through the sides.

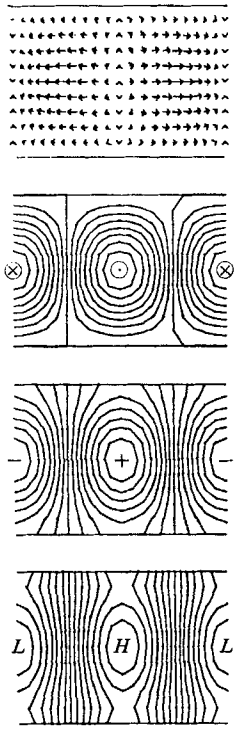

FIGURE 5

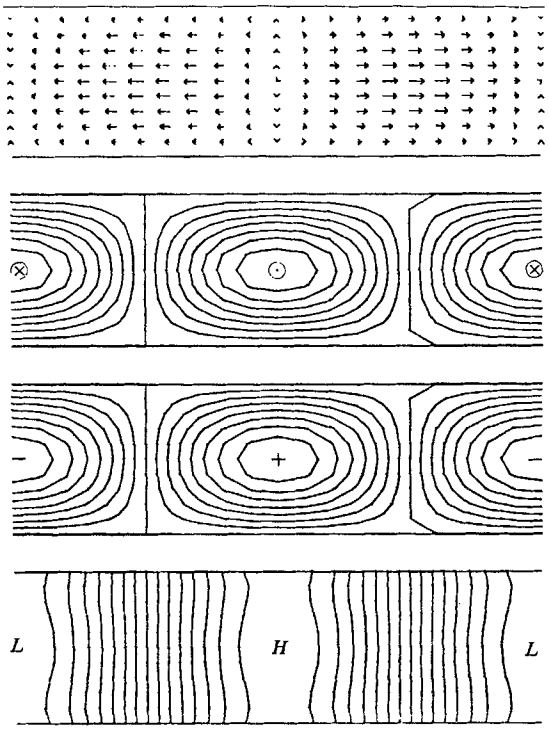

FIGURE 6

FIGURE 5. Horizontal plan form of the cells at the onset of convection for conducting sidewalls and $A = 0{\cdot}5$. Abscissa, x; ordinate, y. From top to bottom: horizontal velocity vectors, isopleths of vertical velocity, isotherms, and isobars for the top half of the channel.

FIGURE 6. Horizontal plan form of the cells at the onset of convection for conducting sidewalls and $A = 2{\cdot}0$.

8. Conclusions

We have shown that although finite rolls aligned perpendicular to rigid sidewalls are not exact solutions of the linearized Boussinesq equations, they closely approximate the preferred modes of convection in infinite channels through a large range of aspect ratio. These results suggest that the upper bounds to the critical Rayleigh number given by Davis (1967) for convection in a box should be accurate in most cases.

We plan to extend this work by including the effects of Coriolis forces due to rotation about a vertical axis. We expect to find that the interaction between the

convective motions and the rotation will sustain a differential rotation through the actions of non-zero Reynolds and thermal stresses.

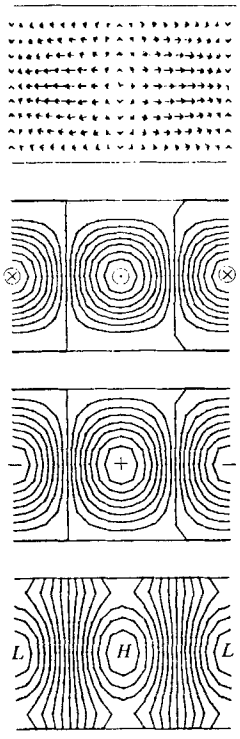

FIGURE 7

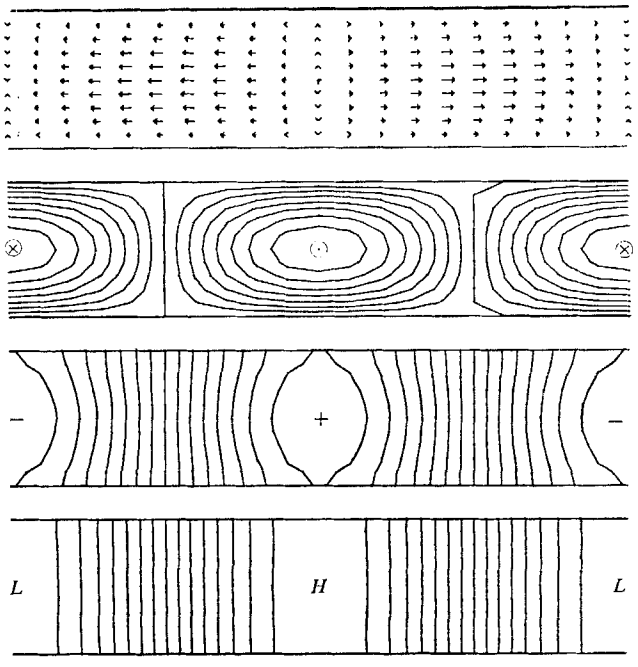

FIGURE 8

FIGURE 7. Horizontal plan form of the cells at the onset of convection for insulating sidewalls and $A = 0{\cdot}5$.

FIGURE 8. Horizontal plan form of the cells at the onset of convection for insulating sidewalls and $A = 2{\cdot}0$.

Computations were performed on the CDC 6400 of the University of Colorado Graduate Computing Center and on the CDC 6600 at the National Center for Atmospheric Research. This research was supported in part by the Air Force Cambridge Research Laboratory, Office of Aerospace Research, under contract F 19628-67-C-0304, but does not necessarily reflect endorsements by the sponsor.

Part of this work is contained in the author's Ph.D. thesis completed at the University of Colorado under the guidance of Dr Peter A. Gilman. His advice and encouragement throughout this work were greatly appreciated.

The National Center for Atmospheric Research is sponsored by the National Science Foundation.

REFERENCES

DAVIS, S. H. 1967 *J. Fluid Mech.* **30**, 465.

INCE, E. L. 1956 *Ordinary Differential Equations*. New York: Dover.

KOSCHMEIDER, E. L. 1966 *Beitr. Phys. Atmos.* **39**, 1.

SEGEL, L. A. 1969 *J. Fluid Mech.* **38**, 203.

SHERMAN, M. & OSTRACH, S. 1966 *J. Fluid Mech.* **24**, 661.